DESIGN OF HWR AT RISP*

G.T. Park†, H.C. Jung, and H.J. Cha,
Rare Isotope Science Project (RISP), Daejeon, Korea

Abstract

We report out progress in developing halfwave resonator (HWR) in RISP. HWR development in Rare Isotope Science Project(RISP) is in its early stage with much effort focused on the cavity design. It aims to deliver various kinds of ions in high current, which requires a large beam pipe aperture ($r = 2\,\text{cm}$), tolerant time transit factor, and the small pressure sensitivity. We present the design of HWR that satisfies above conditions with the optimal performance, including the simulation results on RF design, elctromechanical design, tuning system, and multipaction.

INTRODUCTION

At RISP, a driver linac has a section SCL1-2 consisting of the HWR's that accelerates the low-medium velocity ions. Earlier study on beam dynamics [1] determined the operation condition of the HWR as $\beta = 0.12, f = 162.5\,\text{MHz}$. For uranium $U^{+33}_{235}, U^{+34}_{235}$, it is designed to accelerate from 2.5 MeV/u to 18.52 MeV/u, requiring about 120 HWR's with the accelerating voltage $V_{acc} \sim 1\,\text{MV}$.

In this paper, we present out initial design of the HWR including EM design, mechanical design, multipaction,and sub-system integration.

EM DESIGN SPECIFICATION

The electromagnetic design of the HWR was done by tuning the geometrical parameters of the cavity to optimize the figures of merits. Fig.1 is the finalized EM design of the HWR.

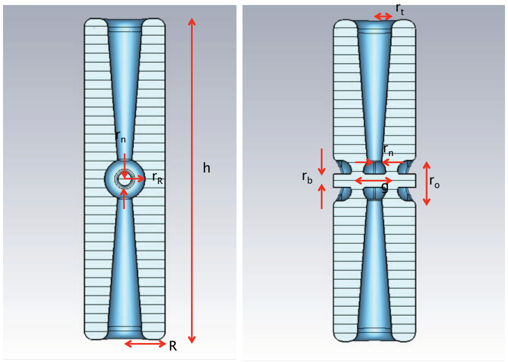

(a) Front view (b) Side view

Figure 1: The sectional view of the HWR.

Table 1,2 list the specifications of EM design obtained with the simulations by 3D solver CST-MWS.

Table 1: The Optimized Geometrical Parameters of the HWR

Geometrical parameters	value (mm)
Total height h	948
Outer radius R	120
Inner top radius r_t	50
Neck size r_n	22
Beam port inner radius r_b	20
Beam port outer radius r_o	60
Gap distance g	35
Gap-to-gap distance d	100

Table 2: Optimized Figures of Merit

figures of merit	value
β	0.12
U(J)	3.93
$G(\Omega)$	4.98
R/Q_0	314.1
V_{acc} (MV)	1.09
E_{peak}(MV/m)	30
B_{peak}(mT)	38.47
P(W)	1.8

U is the stored energy by the electromagnetic field inside the cavity, $G = R_s Q_0$ a geometrical factor with R_s resistivity of the Nb, Q_0 unloaded quality factor, R shunt impedance, V_{acc} the effective accelerating voltage with the time transit factor accounted, E_{peak} the peak electric field, B_{peak} peak magnetic field, and P is power loss at the cavity wall.

In Table 2, the stored energy was determined so that the E_{peak} does not exceed the threshold value$\sim$30 MV/m. Also the effective accelerating field is defined as

$$E_{acc} = V_{acc}/L_{eff} = 4.95\,\text{MV/m}, \qquad (1)$$
$$\text{where } L_{eff} = \beta\lambda = 0.222\text{m}$$

We comment on some features of the design in the optimization. First, the ratio of the outer to inner radius of the cavity was determined to roughly minimize the E_{peak}, B_{peak} values. Secondly, the electric field region (near the beam port) was optimized with the various factors. The donut shape of beam tube was introduced to ensure symmetric quadrupole fields [**?**]. A flat surface was included in the beam port cup to tune the frequency within elastic deformation of the beam port. The blending radius of the surfaces in the beam ports and tube were determined to further improve time transit factor. For easier and cheaper fabrication, the neck region (joining the center

---

* Work supported by ...

† gunnpark@ibs.re.kr

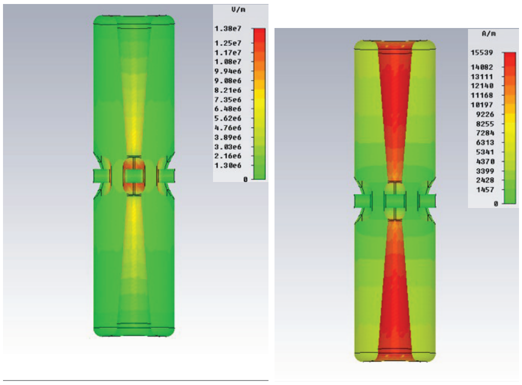

(a) E-field distribution (b) H-field distribution

Figure 2: Electromagnetic field distribution of the HWR

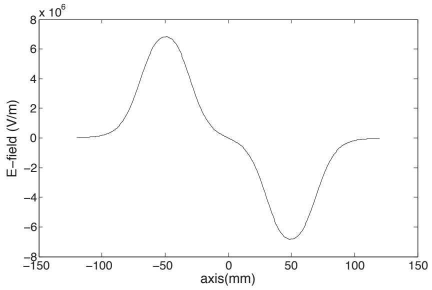

(a) Longitudinal E-field along the axis

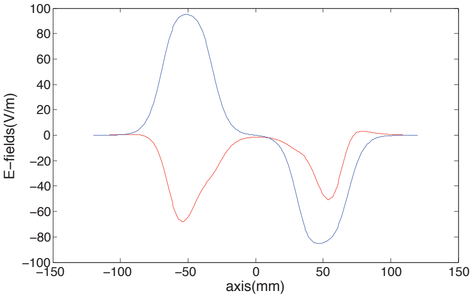

(b) Transverse E-fields along the axis

Figure 3: Longitudinal and transverse electric fields along the beam axis. Black, red, blue lines represent E_x, E_y, E_z fields on the axis, respectively

conductor to the beam tube) was realized by a very short straight section. Finally the magnetic field region (near the short plates) was optimized by tapering the center conductor to further reduce the B_{peak}. Also, the center conductor was joined to the short plates through a straight section (∼9-12.7 mm) for easier e-beam welding.

Fig.6 shows the electromagnetic fields in the cavity.

In particular, Fig.5 shows us the asymmetry of the transverse quadrupole electric fields around the beam axis are negligible, due to the axis-symmetric donut shape of the beam tube.

The error analysis shows that the the margin of the errors in concentricity of the beam axis is more stringent for the transverse fields. For 10% change in asymmetry of the transverse fields, the errors at the beam port must be less than 0.1 mm, which is within engineering control.

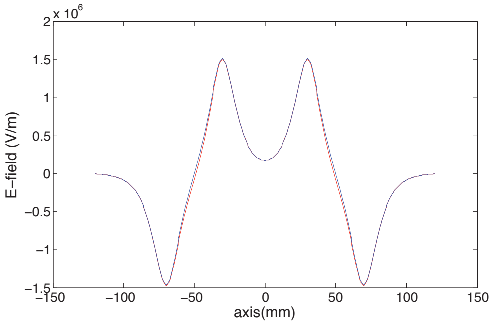

Figure 4: Quadrupole electric field around the beam axis. Red, blue lines represent E_y, E_z fields at $(y, z) = (10, 0), (y, z) = (0, 10)$, respectively

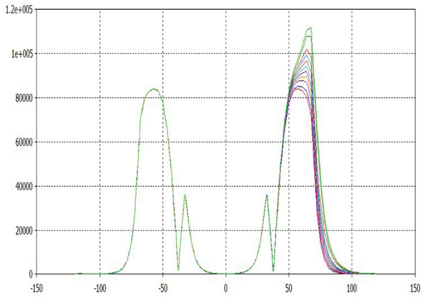

Figure 5: The plot of the difference between E_y at $(y, z) = (10, 0)$ and E_z fields at $(y, z) = (0, 10)$ with the different beam port errors in concentricity.The (lower) green lines are with perfect concentricity.

MECHANICAL DESIGN SPECIFICATION

The degradation of RF performances of the HWR by the various deformations of the cavity from its EM design were identified and studied by the simulations using CST-MPhysics. In particular, the optimized input power to maintain the constant accelerating voltage is computed to increase by 1% for about 0.59 Hz frequency shift [2]. We are planning our rf system to have 30% margin, allowing ±20 Hz bandwidth.

In the simulations, it was assumed that the beam ports are fixed by the tuner via the helium vessel and to reduce the stresses and minimize the deformation, the short plates are stiffened by the rings. Also we assume that the effects of the all the other ports are negligible and the thickness of the cavity wall was determined to be 3 mm.

First, we examined the stresses on the cavity by the evacuation and cool down of the cavity. (The Lorentz pressure in CW operation and Helium pressure cause negligible stresses) At the room temperature, the beam ports were set free, while at cryogenic temperature, the ports were fixed. The results of the simulation are summarized in Table 3. The allowable stresses (for high RRR niobium) based on the yield strength (or the tensile strength) are 25.5 MPa at room temperature and 211.7 MPa at 2 K, respectively. [3] Next, the result for the frequency shift is summarized in Table 4. A electron-beam welding shrinks the HWR by 0.58mm. Chemical polishing usually etches out the surface by 125μm. The beam port was set free in the evacuation simulation. The Lorentz detuning coefficient $K_L = \Delta f/E_{acc}^2$[Hz/(MV/m)^2] is 0.83 Hz/(MV/m)^2. In particular, the main source of the microphonics, helium pressure fluctuation expected to be less than 1 mbar, would set the pressure sensitivity df/dp to be 5.9 Hz/mbar for 10% increased power. In order to minimize the helium pressure sensitivity, we used the fact that the magnetic region (near short plates) shrinks (vertically) with the frequency increase, while the electric region (near beam port) shrinks (axially) with the frequency decreased.(see Fig. 6) Then one can achiev the minimum df/dp by controlling the deformation with the stiffeners such as the ring on the short plates and the re-entrant nose doublers.

Table 3: Stress Anaysis of the HWR.

Process	stress (MPa)
Evacuation (1bar, RT)	29.6
Cool down (2K)	205
Helium pressure (4bar, 2K)	206

Table 4: The Frequency Shift by Various Deformation of the HWR.

Trimming	-150.3 kHz/mm
Surface polishing	94.3 kHz/0.1 mm
Evacuation	-9.8 Hz/mbar
Cooling down (to 2K)	382.8 kHz
Lorentz pressure	-236.2 Hz
Helium pressure sensitivity	-3.8 Hz/mbar

Finally, the mechanical resonant modes were obtained to check they are well above 60 Hz, an upper limit of the various microphonics of the cavity.

SUB-SYSTEM INTEGRATION

Coupler

The capacitive power coupler and the pick up will be implemented to the HWR. (See Fig.5). The specification of the coupler includes the input power P and external quality factor Q_e, whose values are determined assuming the synchronous phase $\phi = 0$ and the beam current $I_{beam} = 0.7$ mA for uranium.

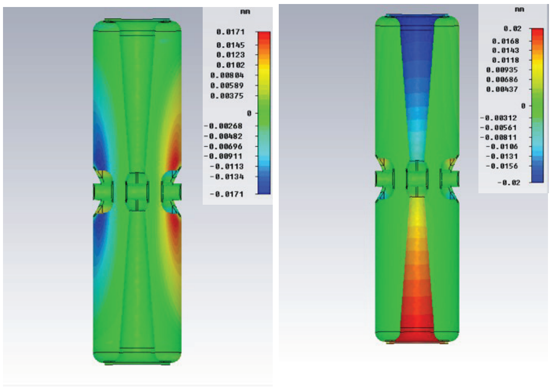

(a) axial deformation (b) vertical deformation

Figure 6: The deformation of the HWR in helium pressure

Table 5: The Specification of the Coupler

Input power	2 kW
Q_{ext}	4.06×10^6
Characteristic impedance	70 Ω
Antenna penetration	-3.8 mm
Frequency shift	600 Hz

Tuner

The slow tuner is implemented so that the tuning force is applied on the flange in the beam port. The tuning range R and the tuning force F are related by the stiffness k and the (tuning) sensitivity s.

$$R = \frac{s}{k}F, \tag{2}$$

The simulation determines $k = 5.08$ kN/mm, $s = -0.4288$ MHz/mm and we would need $\sim$ 1.2 kN to have 100 kHz tuning range.

ACKNOWLEDGMENT

Special thanks go to Hyung Jin Kim and Dong-O Jeon, who guided us to learn and conduct the research on this project. This work was supported by the Rare Isotope Science Project which is funded by the Ministry of Science, ICT and Future Planning (MSIP) and the National Research Foundation (NRF) of the Republic of Korea under Contract 2011-0032011.

REFERENCES

[1] Rare Isotope Science Project, *Baseline Design Summary*, 2012.

[2] A. Neumann et al., Phys. Rev. ST-AB. 13 (2010) 082001.

[3] Fermi lab report, *Niobium properties*, p. 112

[4] P.N. Ostroumov et al., "Development of a half-wave resonator for project X," WEPPC039, Proceedings of IPAC2012, New Orleans, Louisiana, USA.